

OPEN ACCESS

Fiber Bragg sensing of high explosive detonation experiments at Los Alamos National Laboratory

To cite this article: G Rodriguez *et al* 2014 *J. Phys.: Conf. Ser.* **500** 142030

View the [article online](#) for updates and enhancements.

Related content

- [Ultra dispersed mixture of PETN and RDX for explosive welding](#)
K A Ten, E R Prueel, A O Kashkarov *et al.*
- [Joining of tubes by gas detonation forming](#)
Vahid Jenkouk, Sandeep Patil and Bernd Markert
- [Transverse initiation of an insensitive explosive in a layered slab geometry: initiation modes](#)
E K Anderson, T D Aslam and S I Jackson

Recent citations

- [Review of Chirped Fiber Bragg Grating \(CFBG\) Fiber-Optic Sensors and Their Applications](#)
Daniele Tosi
- [Ultrafast Fiber Bragg Grating Interrogation for Sensing in Detonation and Shock Wave Experiments](#)
George Rodriguez and Steve Gilbertson
- [Spectral response of multilayer optical structures to dynamic mechanical loading](#)
David Scripka *et al*



IOP | ebooks™

Bringing you innovative digital publishing with leading voices to create your essential collection of books in STEM research.

Start exploring the collection - download the first chapter of every title for free.

Fiber Bragg sensing of high explosive detonation experiments at Los Alamos National Laboratory

G Rodriguez¹, R L Sandberg¹, S I Jackson², S W Vincent², S. M. Gilbertson¹ and E Udd³

¹Materials Physics and Applications Division, Los Alamos National Laboratory, Los Alamos, New Mexico 87545 USA

²Weapons Experiments Division, Los Alamos National Laboratory, Los Alamos, New Mexico 87545 USA

³Columbia Gorge Research LLC., Fairview, OR 97024 USA

E-mail: rodrigeo@lanl.gov

Abstract. An all optical-fiber-based approach to measuring high explosive detonation front position and velocity is demonstrated. By measuring total light return using an incoherent light source reflected from a fiber Bragg grating sensor in contact with the explosive, dynamic mapping of the detonation front position and velocity versus time is obtained. We demonstrate two examples of detonation front measurements: PETN detasheet test and detonation along a multi-HE cylindrical rate stick containing sections of PBX 9501, Comp B, TNT, PBX 9407, PBX 9520, and inert PMMA. In the PETN detasheet measurement, excellent agreement with complementary diagnostics (electrical pins) is achieved, with accuracy in the detonation front velocity at the 0.13% level when compared to the results from the pin data.

1. Introduction

Fiber Bragg grating (FBG) sensors are proving to be a valuable diagnostic for detonation and shock sensing [1, 2]. They provide very good detonation and shock tracking performance when compared to other established methods such as electrical pins, optical streak camera recording, or velocimetry. These sensors can be attached to inert and high explosive (HE) materials as surface or embedded probes, and because they operate in detonation and/or shock environments, their versatility makes them attractive as dynamic sensors in detonation and shock events of materials that are otherwise difficult to diagnose using surface-only probes. At Los Alamos, we have applied the technology to develop a diagnostic baseline for both HE detonation and shock velocity measurements. In the HE detonation case, we seek to establish confidence levels in the approach by performing measurements that attempt to determine precision and response speeds. The HE detonation measurements are aimed at demonstrating precision through comparison with complementary diagnostics, and are also aimed at determining response times by making measurements in cases where the detonation velocity is expected to vary, such as in a situation where multiple explosives are used. We also aim at testing FBGs where the total burn distances are long, *i.e.*, tens of centimeters. With temporal resolution currently at the ten nanosecond level, we have applied FBG sensing to the following tests: detonation tracking up to a ~200 mm long run using concatenated FBGs, detonation across multiple boundaries of differing HE types, and detonation-to-shock tracking across an HE/inert material interface.



2. Methods

The detonation velocity detection system is described in detail elsewhere [2], and we give a brief description here. A block diagram of the experimental setup is shown in figure 1. We use an incoherent broadband amplified spontaneous emission (ASE) source centered about the well-known telecommunication C-band (1525 nm - 1565 nm). Light from the ASE light source is launched into a single-mode fiber system and then to a 3-port power circulator. The power circulator directs light to the embedded chirped FBG (CFBG) sensor at port 2. The CFBG sensor consists of a linearly chirped grating written along a predetermined length of bare SMF-28 with maximum reflectivity within the C-band. Detonation wave tracking is accomplished using the sensor by being in direct contact (embedded or surface) with the HE. As the HE detonation wave travels along the length of the sensor, the fiber's index of reflection is first modified by the intense shock driven into the fiber by the adjacent high-pressure detonation products as the wave propagates axially along the grating's length. In rapid succession, the grating is consumed by the high temperatures and pressures associated with this event. Shock-processed portions of the grating no longer transmit/reflect light due to substantial modification to the local index of reflection and damage of the grating structure. Since spectral encoding of the CFBG wavelength reflection band is linear with length (linear chirp), propagation of a detonation axially along the fiber grating continuously and linearly reduces the reflected grating bandwidth as a function of time. Thus, the detonation phase velocity along the fiber axis can be measured by a CFBG embedded in the HE or placed at various boundaries capable of accommodating the bare 150- μm -diameter fiber (125 μm for cladding with 25 μm of recoating, typically polyimide). For our experiments, power levels launched into the CFBG detonation velocimetry system were typically 0.0 dBm (1 mW). Near complete total reflection (> 90% light return) off the CFBG occurs along the detection leg of the system. After reflecting off the CFBG, the reflected light is directed through the power circulator at port 2, where only reflected light off the CFBG is detected at the circulator output port (port 3) using a fast (125 MHz BW) InGaAs photodetector. Dynamic recording of the event is done with a fast recording digitizing oscilloscope. The current bandwidth of the measurement system is limited by the response time of the photodiode.

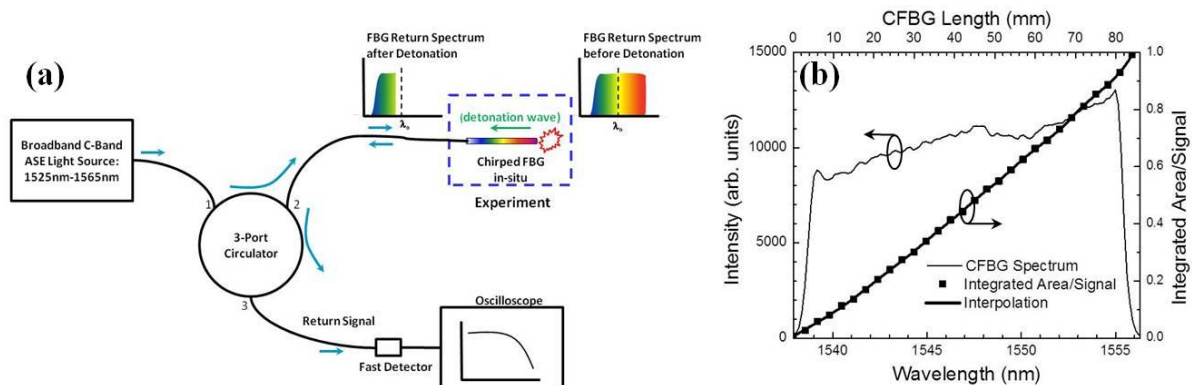


Figure 1. (a) Chirped fiber Bragg (CFBG) detonation detection system, and (b) an example showing the spectrum of an 85-mm long CFBG sensor. The square symbol-line plot is the integrated area plot of the CFBG power as a function of length (wavelength) according to equation (1).

Transformation from the experimentally recorded trace of voltage versus time at the detector is related to the length/position versus time response function of the grating after data reduction. The grating reflection bandwidth is centered at 1550 nm, but is less than the bandwidth of the ASE light source so that the flattest spectral portion of the ASE source overlaps with the grating reflectance band. The reflected intensity, R , is proportional to the integrated return light spectrum off the grating. However, since encoding of grating length versus wavelength is linear, R is linearly proportional to L and λ , provided that the grating reflected spectrum produced by the ASE light source can be assumed to be an idealized flat-top. In general, the integrated light return voltage signal is,

$$R(t) = a \int_{\lambda_1}^{\lambda_2(t)} S_G(\lambda) ASE(\lambda) d\lambda \quad (1)$$

where, a is a normalization constant, $S_G(\lambda)$ is the grating reflection spectrum, $ASE(\lambda)$ is the light source spectrum, and λ_1 and λ_2 are the lower and upper wavelength limits, respectively. Here we assume λ_2 is the wavelength position where the detonation wave is located, *i.e.*, $L(t) \propto R(t)$, and λ_1 corresponds to the shortest wavelength reflected by the grating, which is located nearest to the light source. We also assume that the photodiode has a flat spectral response across the CFBG reflectance band. Data analysis yields time-of-arrival data $L(t)$ for a detonation propagating along the CFBG sensor. The temporal derivative of $L(t)$ computes the local detonation phase velocity along the fiber.

3. Results

In this paper we report on two detonation example tests utilizing CFBGs. The first test is a single HE detonation run along a PETN detasheet diagnosed by two concatenated 100-mm-long CFBGs and by a set of electrical wire pins. The second example is a cylindrical rate stick comprised of multiple HE types diagnosed by seven CFBGs (two 100 mm and five 10 mm CFBGs).

A photograph of the PETN detasheet test is shown in figure 2. A linear detonation run of approximately 200 mm is diagnosed by concatenating two 100 mm long CFBGs and by ten electrical wire pins. The entire length of the detasheet is 381 mm. The zero position is referenced from the break out end on the left side in figure 2. The pin number and positions in mm were: (1) 184.78 mm, (2) 166.10 mm, (3) 147.77 mm, (4) 129.33 mm, (5) 110.75 mm, (6) 92.21 mm, (7) 73.73 mm, (8) 55.35, (9) 36.82 mm, and (10) 18.41 mm. The CFBG number end positions were located at: CFBG1 205.05 mm and CFBG2 107.74 mm. Figure 3 is a plot of the results from this test with linear fits showing the extracted velocities for the pins and CFBGs. Due to a failure of the impedance termination of pins 8, 9 and 10, only pins 1 thru 7 returned valid data. Nonetheless, agreement between the two is excellent with a least squares fit and error of 7.068 ± 0.0012 mm/ μ s and 7.059 ± 0.007 mm/ μ s for the CFBG and pin measurement, respectively. The results demonstrate that over runs as long as 200 mm that CFBGs yield comparable accuracy, and it is expected that the FBG approach may be more desirable under conditions requiring embedded sensors or when rapid velocity changes are expected where a time continuous type measurement would be preferred.

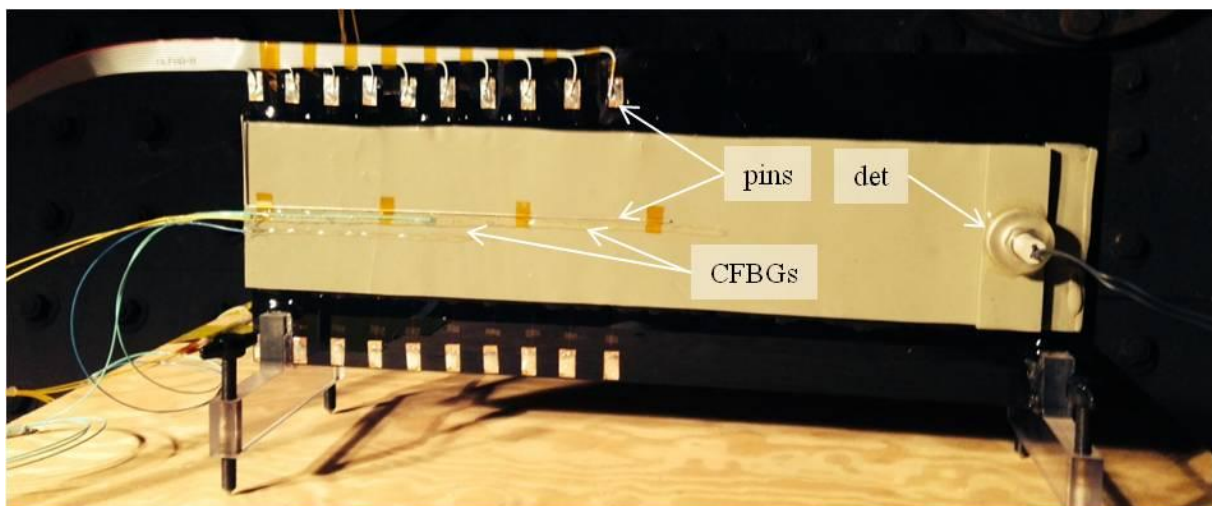


Figure 2. Photograph of the PETN detasheet test. An RP-1 detonator on the right initiates the charge and subsequent detonation wave moving to the left is diagnosed by ten electrical pin wires and two 100 mm CFBGs. Registration of the placement position of the pins and fiber sensors are referenced to the end breakout position on the left end.

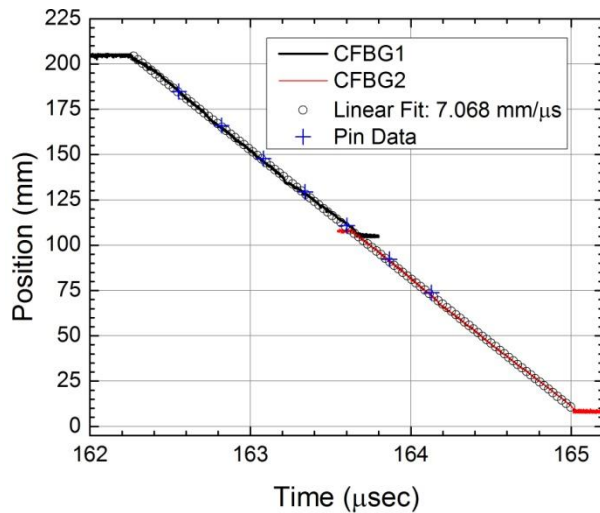


Figure 3. Plot of the PETN detasheet detonation burn front position versus time for the CFBG and electrical pin measurements. Two 100-mm long CFBGs are concatenated to achieve a total run length of 200 mm. A linear least squares fit to the CFBG data is shown as open circles in the plot. The least squares fit to the CFBG and pin data yield a detonation velocity of 7.068 mm/ μ s and 7.059 mm/ μ s for the CFBG and pin data, respectively.

For the second example, a rate stick test comprised of multiple HE types was used to test the sensitivities of two different CFBGs, each with a different linear chirp rate. The goal was to test spatiotemporal sensitivity effects by combining a measurement where the expected detonation velocity differences (by using different HE materials) can be simultaneously tracked with two CFBG with different linear chirps. In figure 4 we show an illustration of the HE assembly and the locations of CFBGs fielded. A 12.7-mm-diameter and 154.3-mm-long cylindrical rate stick consisting of five 25.4-mm-long sections of different HE materials (PBX 9501, Comp B, TNT, PBX 9407, PBX 9502) and one 25.4-mm-long section of inert PMMA plastic was fielded for the test. The assembly was initiated by an RP-1 detonator. Test diagnostics included two 100-mm-long CFBGs and five 10-mm-long CFBGs for detonation velocity determination. The CFBGs were glued (M-Bond 200 epoxy) at the positions shown in figure 4. The 100-mm and 10-mm CFBG spectra are shown in figures 4(b) and 4(c), and they had a measured chirp of 0.35 nm/mm and 3.5 nm/mm, respectively.

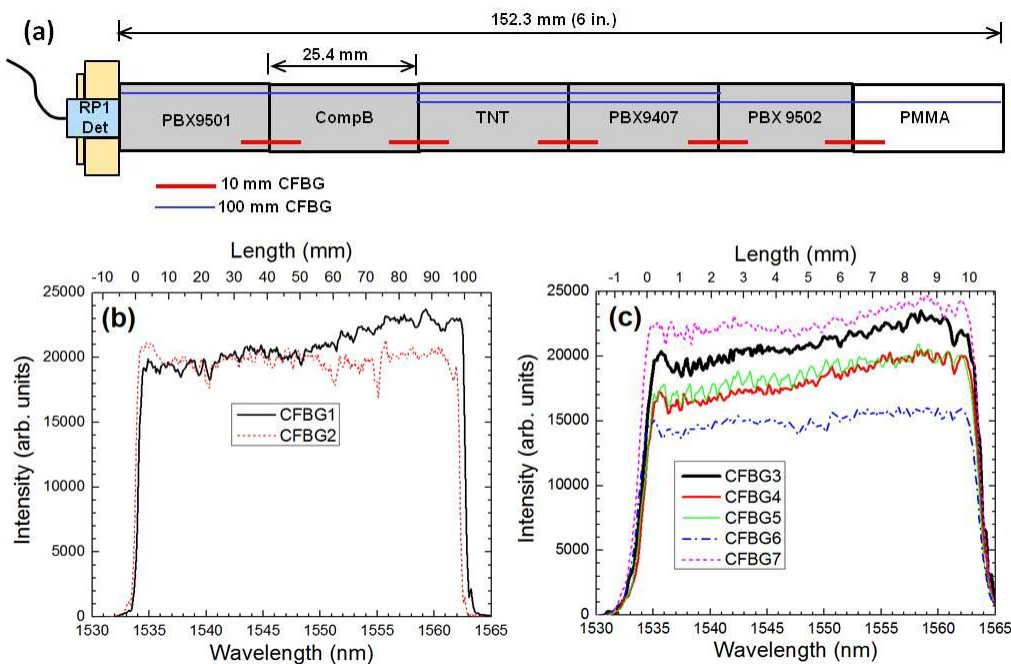


Figure 4. (a) Illustration of the multi-HE rate stick experiment and corresponding CFBG spectra for the (b) 100-mm-long and (c) 10-mm-long sensors. The illustration does not show that the CFBGs had to be placed at varying azimuth angle to minimize fiber optic cabling interference.

Table 1 below lists the length, position, and material mapping for the seven CFBGs used in the test. The objective is to catalog differences in the performance of the long (100 mm) CFBGs versus the short (10 mm) with respect to the ability to record sudden changes in detonation velocity. The results are shown in figure 5 for the 100-mm and 10-mm CFBGs.

Table 1. CFBG sensor lengths, position, and material placement used in the multi-HE rate stick test.

CFBG Sensor	Length (mm)	Position (mm)	Material Interface(s)
1	100	0.54	PBX 9501/Comp B/TNT/PBX 9407
2	100	50.7	TNT/PBX 9407/PBX 9502/PMMA
3	10	20.1	PBX 9501/Comp B
4	10	45.9	Comp B/TNT
5	10	70.7	TNT/PBX 9407
6	10	96.2	PBX 9407/PBX 9502
7	10	121.6	PBX 9502/ PMMA

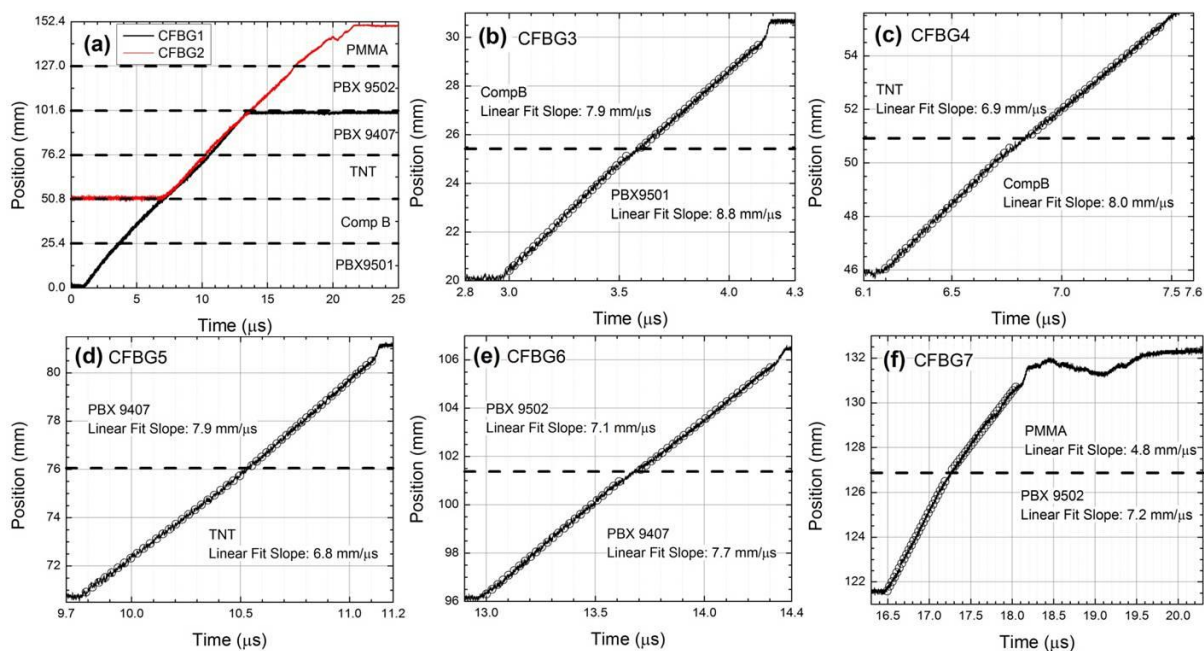


Figure 5. Position versus time results for the multi-HE rate stick test. The two 100-mm-long CFBG results are shown in (a), and five 10-mm-long CFBGs are shown in (b) thru (f). The material boundaries in each plot are designated by dashed horizontal line with the material labeled in each section below or above the dashed line. Linear fits to data for the 10-mm-long CFBG data are shown as circle symbol plots in (b) thru (f), and the slope yielded velocities as labeled in each graph. These are also listed in table 2. Also note that in (f), a shock wave is launched into the inert PMMA plastic is measured at 4.8 mm/μs.

Comparing the results between two sets shows a slight difference in the ability of CFBGs to detect abrupt changes in slope (velocity) between material interfaces. The 10-mm CFBGs appear to better track the change at the interface as a result of their better spatial resolution, and we determine that the response time is sub-50 ns to changes in slope (velocity). This limit, however, may not be intrinsic to the CFBG detection system, but possibly a function of the disruption in the burn front and material

flow across a boundary between different HE materials. For example, for a detonation front traveling at 7 mm/ μ s, in a 50 ns window the front has travelled \sim 350 μ m, and this distance may not sufficient for establishing a steady flow across reactive boundaries. Further tests with faster velocity changes are necessary establish the time resolution limit of CFBGs for detonation velocity measurements. Table 2 lists the accepted and measured values for the detonation measurements made in this test. The last column is the experimentally measured averaged detonation velocity as measured by the average of the two 10-mm CFBGs that were placed on each HE. Finally, it also important to briefly highlight the shock velocity as measured in the transition between PBX 9502 and the inert PMMA plastic. The shock impedance mismatch between the zones accounts for the reduction of the shock velocity launched into PMMA, and demonstrates the CFBG ability to track shock position, provided the shock pressure is high enough to extinguish light return from the CFBG as it travels along the sensor. The ringing in the signal at the near the end of record in the PMMA (figure 6(f)) is indicative of an attenuating pressure shock that appears to disrupt the sensor (but not destroy it) after a few mm of propagation into the material.

Table 2. List of the accepted and measured HE detonation velocities from the multi-HE rate stick test.

HE Material	Detonation Speed (mm/ μ s)	Avg. Measured Speed with 10-mm CFBG (mm/ μ s)
PBX 9501	8.8	8.8
Comp B	8.1	8.0
TNT	6.9	6.9
PBX 9407	8.0	7.8
PBX 9502	7.6	7.2

4. Conclusions

FBG sensors are being developed and deployed for use in high explosive and shock wave science experiments. Two tests are demonstrated where linearly chirped fiber Bragg gratings are used to measure detonation front position (and velocity) versus time. In the PETN detasheet test, we show that a detonation along single-HE burn results in a velocity accuracy of the CFBGs to 0.13% when compared to the pin data. In the detonation involving multiple-HE materials, we show that gratings with larger chirp rates have better sensitivity to changes in velocity. The results for 10-mm (chirp: 0.35 nm/mm) gratings compared to 100-mm (chirp: 3.5 nm/mm) gratings show that changes in *velocity* are better tracked (sub-50 ns) by the 10-mm gratings because of the better spatial resolution than the 100-mm gratings. However, the fastest time resolution is still yet to be determined as the tests conducted have not tested the ultimate limit of the grating or detection system.

Acknowledgments

This work is funded at the Los Alamos National Laboratory under the auspices of the Department of Energy for Los Alamos National Security LLC under Contract no. DE-AC52-06NA25396.

References

- [1] Benterou J, Bennett C V, Cole G, Hare D E, May C, Udd E, Mihailov S J and Liu P 2009 *SPIE* **7316** 73160E
- [2] Rodriguez G, Sandberg R L, McCulloch Q, Jackson S I, Vincent S W and Udd E 2013 *Rev. Sci. Instrum.* **84** 015003